Ab initio study of deuterium in the dissociating regime: Sound speed and transport properties

J. Clérouin*
Commissariat à l'Energie Atomique/DIF, Département de Physique Théorique et Appliquée, Boîte Postale 12, 91680 Bruyères le Châtel Cedex, France

J.-F. Dufrêche†
LI2C, Université Pierre et Marie Curie, Case Courrier 51, Bâtiment F, 4 Place Jussieu, 75252 Paris Cedex, France
(Received 27 June 2001; published 26 November 2001)

The sound speed and the transport properties of dense hydrogen (deuterium) are computed from local spin-density approximation molecular-dynamics simulations in the dissociating regime. The sound speed c_s is evaluated from the thermodynamical differentiation of the equation of state in the molecular phase and is in very good agreement with recent experiments. The diffusion constant D and the viscosity η are extracted from simulations performed at $V=6$, 4, and 2.7 cm^3/mole, corresponding, respectively, for deuterium at $\rho=0.672$, 1.0, and 1.5 g/cm^3 in a range of temperatures 1000 K$<T<$50 000 K. In the dissociated regime, the diffusion coefficient is well predicted by one-component plasma formulas using a renormalized coupling parameter recently proposed by Murillo [M. S. Murillo, Phys. Rev. B **62**, 4115 (2000)]. The behavior of the shear viscosity in the dissociated regime is more complex and exhibits a crossover between atomic and screened plasma formulation. A comparison with recent molecular-dynamics simulations of Yukawas systems shows that the inverse of the screening length must lie between 1 and 2, in nearest-neighbor radius units, as suggested by the results on the diffusion.

DOI: 10.1103/PhysRevE.64.066406 PACS number(s): 52.25.Fi, 61.20.Ja, 71.15.Pd

I. INTRODUCTION

In a previous paper [1] we reported local spin-density approximation (LSDA) molecular-dynamics simulations of deuterium, which confirmed the discrepancies between *ab initio* simulations [2–4] and experimental results on the hugoniot [5–7]. In particular, the calculated compressibility ($\rho/\rho_0 \simeq 4.4$) appeared much smaller than predicted by the experiments ($\rho/\rho_0 \simeq 6$). Nevertheless, the good agreement between LSDA results and theoretical predictions observed in the deep molecular phase as well as in the fully dissociated regime suggest that most of the the physics is captured by those simulations, and encouraged us to compute more precisely physical quantities of interest.

The goal of this paper is to compute transport properties of hydrogen with a special emphasis on the dissociated regime. Transport properties of dense hydrogen have been the subject of many studies, each addressing specific regions of the phase diagram. As a first approach, the very dense hydrogen plasma regime ($T>100\,000$ K, $\rho>2$ g/cm^3) can been interpreted on the basis of the one-component plasma (OCP) properties and OCP fits can be used to evaluate the diffusion constant [8] and the viscosity [9]. This limiting case corresponds to a very high electronic density characterized by $r_s=a/a_B \ll 1$, where a_B is the Bohr radius, $a=(3/4\pi n)^{1/3}$ is the mean ionic sphere radius, and n is the number density. To describe more accurately partially degenerate systems, screening has been introduced self-consistently beyond linear response through Thomas-Fermi statistics with the Thomas-Fermi molecular-dynamics model [10,11] and his effect on diffusion has been quantified at $r_s=1$ corresponding to a density of 2.6 g/cm^3. In this regime, Kohanoff and Hansen [12] computed the properties of the dense plasma using *ab initio* simulations in the local density approximation, and Kwon *et al.* [13] investigated the region $2<r_s<1$ by means of tight-binding molecular-dynamics simulations, allowing for the recombination of hydrogen atoms into molecules. The effect of finite electronic temperature was introduced by Alavi *et al.* [14] who computed the sound speed in the interior of Jupiter ($1<r_s<1.3$). From a more formal point of view, there have been many publications on the thermodynamics of Yukawa systems initiated by Robbins *et al.* [15], Farouki *et al.* [16], and more recently by Caillol and Gilles [17]. The question of Ewald summations for screened potentials, which was put apart before, has been solved by Rosenfeld [18] and also by Salin and Caillol [19] allowing for accurate results for self-diffusion [20] and for viscosity [21]. The effect of the screening on transport properties has recently received a simple response by Murillo who suggested a recipe to extend the results of the OCP to the screened system [22]. Lower densities ($r_s=2$) and lower temperatures $T<10\,000$ K address the problem of the dissociation of hydrogen and the transformation from a screened plasma to a dense molecular fluid. This question, which is also at the heart of the problem of the hydrogen equation of state, is still unresolved and has motivated numerous simulation studies [2,3].

This paper is organized as follows. First we detail the *ab initio* model used and particular settings. A classical model designed to compute, for a low cost, transport properties in the molecular-atomic transition regime, is briefly described. In the next part we propose a simple fit of the computed molecular equation of state (EOS) which incorporates zero-temperature experimental results and allows us to extract the

*Electronic address: jean.clerouin@cea.fr
†Electronic address: dufreche@ccr.jussieu.fr

sound speed in this regime. Diffusion and shear viscosity are then computed from simulations in the last part and compared with our classical dissociation model and screened plasmas models. The predictions of this last model are then compared with results of simulations for a higher density ($r_s=1.5$, $V=2.7$ cm^3/mole corresponding to $\rho=1.5$ g/cm^3 for deuterium) where the transition from molecular to plasma is more sudden and occurs without going through an atomic state.

II. MODELS

The accuracy of the evaluation of the dynamical properties, such as self-diffusion or viscosity, using molecular-dynamics simulations, is strongly correlated to a precise determination of interactions between protons, treated at a classical level. These interactions can be described either by effective potentials, fitted on experimental results, or by first-principle computations of the interactions between protons immersed in a polarizable electronic density. Density-functional theory (DFT) provides the framework of the latter approach through so-called *ab initio* methods that solve the Kohn-Sham equations in various approximations of the exchange correlation (for a review of DFT methods, see [23]). Numbers of computational codes are now available allowing for DFT molecular-dynamics simulations of hundreds of particles in contrast with effective potential methods [classical molecular-dynamics (MD) codes] where millions of particles are now the standard. Because each approach has its own advantages, we tried to use both methods in a complementary way.

A. *Ab initio* simulations

Extensive *ab initio* simulations were performed with the VASP code, which is a plane-wave pseudopotential code developed at the Technical University of Vienna [24]. Vanderbilt ultrasoft pseudopotentials [25] are used with a LSDA functional given by the Perdew-Wang 91 parametrization of the generalized gradient approximation (GGA) (including explicitly the spin) [26]. Simulations from which transport coefficients have been computed, were carried out with 108 atoms. If temperature, pressure, and total energies are well converged after 600 time steps of 0.2 fs of purely microcanonical simulations (after 300 time steps of thermalization by velocities rescaling), more time steps are needed to get statistically significant transport coefficients. The electronic temperature was set equal to the required ionic temperature. The number of electronic states was taken in order to have an occupancy for the highest state, given by the Fermi-Dirac statistics, smaller than 10^{-5}. We have identified three sources of inaccuracies: the number of particles, the pseudopotential cutoff, and the Brillouin-zone sampling. An estimation of size effects has been done by comparing the pressures obtained with 64 and 108 particles. In most cases this difference is of order of 15%, particularly in the dissociation region. Convergence in the the ultrasoft pseudopotential cutoff needs a value of 450 eV. Tests have shown that the pressure is very sensitive to the cutoff and that the use of a 150-eV cutoff would lower the pressure by 30%. Concerning the Brillouin-zone sampling, for $N=108$ atoms, using Gamma point or a mesh of 3^3 points, gives a 5% variation in pressure. We thus have chosen to stay at the Gamma point in order to perform longer simulations (2000–4000 time steps of 0.2 fs for the highest temperature).

B. Classical model

To overcome the difficulty of lengthy *ab initio* simulations we have also devised a simple classical model to understand the effect on transport coefficients of dissociating molecules into atoms. This model [27] performs a classical molecular-dynamics simulation of a mixture of molecules and atoms in a proportion prescribed by the Ross model [28]. Molecule-molecule potentials are given by the Ross-Ree-Young (RRY) potential [29] and the atom-atom potential by an exp-6 potential with short-range corrections [30]. Atom-molecules interactions were given by a Lorentz-Berthelot mixing rule. Molecular-dynamics simulations were performed for 864 particles for 10 000 to 40 000 time steps for a very low cost. From a set of simulations at different volumes, we have computed the viscosity from the stress tensor and after a study based on scaling laws, a universal rule has been given that fits the viscosity values with a reasonable precision:

$$\eta = T^{5/2}\exp[a + b\ln x + c\ln^2 x]\times 10^{-5}\ \text{Pa s}, \qquad (1)$$

where $x=\rho T^{-1/3}$ and $a=38.17$, $b=3.586$, and $c=0.0547$. The overall shape of the predicted viscosities given by the fit (1) (dotted curves in Figs. 7, 8, and 9) exhibits two different behaviors with a minimum around the dissociation temperature. At low temperature, the system behaves as a dense fluid with a decreasing viscosity with temperature (''liquid behavior'') and when dissociation occurs this trend reverses and the viscosity increases with temperature (''gas behavior''). This change is easily explained when considering the two components (kinetic + potential) of the stress tensor. Potential terms are dominating stress-stress correlations at low temperature, and kinetic terms at high temperature. Although this trend can be observed for the OCP model, where the viscosity exhibits a minimum around $\Gamma\simeq 10$, it is strongly enhanced here by the dissociation process.

In the molecular regime, the order of magnitude of the viscosity can be deduced from the diffusion constant through the Stokes-Einstein relation,

$$\eta = \frac{kT}{2\pi\sigma D}, \qquad (2)$$

where σ is a variational diameter and D is the diffusion constant of the molecules, which in this regime identifies with the proton self-diffusion constant. If we take $T=2000$ K, $D=10^{-3}$ cm^2/s from Table III, and $\sigma=1.8$ Å from a variational calculation, we get $\eta\simeq 2\,10^{-4}$ Pa s, which is in excellent agreement with the viscosities at low temperatures in the molecular regime.

At high temperature ($T>2000$ K) the system is mostly atomic (following the Ross model) and the main contribution

TABLE I. Thermodynamic properties of the molecular phase for two densities corresponding to $r_s=2$ ($\rho=0.665$ g/cc) and $r_s=1.75$ ($\rho=1$ g/cc). P_{Fit} is computed using Eq. (3) with $b=0.8$ cm^3/mole.

r_s	Temperature (K)	P_{Pot} (GPa)	P_{Tot} (GPa)	P_{Fit} (GPa)	c_T km/s
2	0			12.7	7.7
	786	14.5	16.7	15.8	8.1
	1350	15.2	19.1	17.9	8.4
	2200	15.3	21.5	21.3	8.8
	3550	16.5	26.4	26.4	9.4
	4090	15.8	27.3	28.4	9.6
	4800	11.9	25.3	31.1	9.8
1.75	0			41.9	10.6
	896	42.3	46.0	44.7	11.1
	1174	45.4	53.8	49.3	11.2
	3031	42.6	55.3	53.6	12.1
	3932	38.5	55.0	57.3	12.5

to the viscosity arises from atom-atom interactions, which are purely atomic; no Coulombic contributions have been introduced (viscosities will be quoted as atomic model in the figures). We expect that this model gives valuable predictions when a well-defined atomic phase exists between the molecular and the plasma phase.

III. MOLECULAR PHASE

The quality of LSDA simulations in the molecular phase can be quantified by the equation state and by its coherence with classical models and experimental results, and also by the dynamical properties of protons revealing vibrational and rotational degrees of freedom of molecules.

A. Thermodynamics

The measured pressures in the molecular phase are given versus temperature for fixed volume in Table I. We have separated the potential contribution P_{Pot} from the total P_{Tot} contributions to show the slowly varying potential contribution in the total pressure before dissociation. It is thus natural to introduce the experimental pressure at zero K obtained by Loubeyre *et al.* [31] as a cold curve, given by the Vinet equation, and to propose a fit in the form

$$P(V,T)=P_0(V)+a(V)*T=P_{Vinet}(V)+\frac{\mathcal{R}T}{V-b}, \quad (3)$$

where b is a covolume and P_{Vinet} is given by

$$P=3K_0\left(\frac{V}{V_0}\right)^{-2/3}\left[1-\left(\frac{V}{V_0}\right)^{1/3}\right] \times\exp\left\{\frac{3}{2}(K_0'-1)\left[1-\left(\frac{V}{V_0}\right)^{1/3}\right]\right\} \quad (4)$$

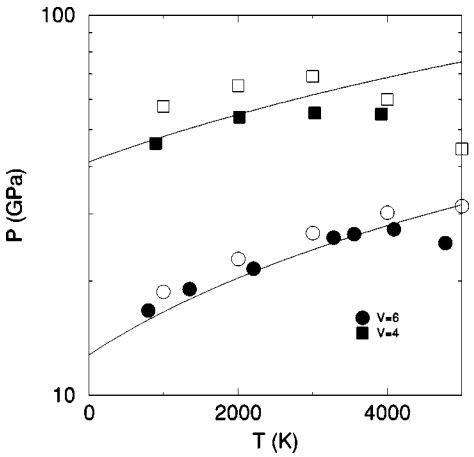

FIG. 1. Fits of pressure versus temperature in the molecular regime. The filled symbols are *ab initio* simulations, lines are given by Eq. (3) with $b=0.8$ cm^3/mole, and open symbols are classical estimations using RRY intermolecular potentials.

with $V_0=25.433$ cm^3/mol, $K_0=1.62$ Kbar, and $K_0'=6.813$ (parametrization given in [31]).

As shown in Fig. 1, pressures computed with the *ab initio* code (filled symbols) are in reasonable agreement with the empirical EOS (3) using a covolume $b=0.8$ cm^3/mole, for the two densities ($V=6$ cm^3/mol and $V=4$ cm^3/mol). Empty symbols represent the pressures computed with the classical model, whose main contribution in this region comes from the RRY potential between molecules. At the lower density ($V=6$ cm^3/mol) classical pressures are in good agreement with the fit (3) but systematically too high at the higher density ($V=4$ cm^3/mol). It is interesting to note that the onset of dissociation is signaled by the sudden diminution of the potential contribution of the pressure.

B. Sound speed

Equation (3) allows us to compute the sound speed at $T=0$ K by taking the derivative of of the Vinet equation with respect to the volume. As shown in Fig. 2 we get a direct evaluation of c_s at 0 K, which is in excellent agreement with the experimental results of Pratesi *et al.* [34] for hydrogen. The same derivation for deuterium (still at 0 K) falls also very close to recent experiments of Holmes [32]. At finite temperature we get c_T by differentiation of Eq. (3), which differs from c_s by a factor of $\sqrt{\gamma}$, γ being the polytropic coefficient, which in this range of densities is between 1.4 and 1.3. This introduces an uncertainty of 10% in our evaluation of c_s. In order to compare with Holmes experiments, we have used the Sesame EOS for deuterium [33] to estimate volume and temperature corresponding to each measurement of the sound speed for a given hugoniot pressure (Table II). By introducing those quantities into Eq. (3) we have deduced the isothermal sound speed which, taking into account a factor of 10% for γ, yields values in excellent agreement with the experiments and also with the Sesame prediction for deuterium (dashed line on 2).

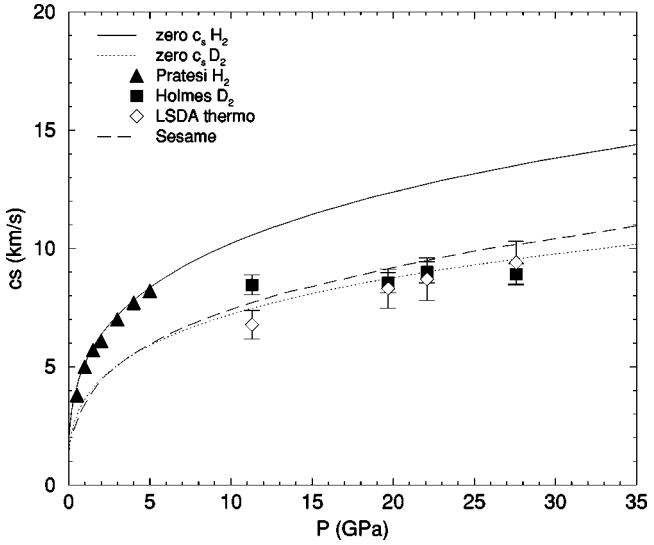

FIG. 2. Sound speed velocity versus pressure evaluated on the principal hugoniot. The filled squares are experimental hugoniot data [32], filled triangles are 0 K diamond anvil cell measurements [34], and empty diamonds with error bars are fitted LSDA results with Eq. (3). The full line is the 0 K derivation of the Vinet equation for hydrogen and the dotted line is the same derivation for deuterium. The dashed line is the Sesame prediction for deuterium [33].

C. Dynamics of the molecular phase

Atomic motion is revealed by the computation of the proton velocity autocorrelation function:

$$Z(t)=\frac{1}{3}\langle v_i(\tau)\cdot v_i(0)\rangle$$

from which by a simple time integration we get the diffusion constant we are going to discuss in the next section. We have plotted in Fig. 3, $Z(t)$ and its Fourier transform $\tilde{Z}(\omega)$ for a pure molecular case $r_s=2$ and $T=1330$ K. Two frequencies are well defined: A high frequency that identifies with the vibrational frequency of deuterium $\omega=0.0138$ a.u. $=3055\ \mathrm{cm}^{-1}$, and a much lower frequency that corresponds to a band of rotational states of the molecule [34].

TABLE II. Pressure and sound speed measured on the principal hugoniot by Holmes [32]. Corresponding thermodynamical conditions are evaluated with Sesame EOS [33] and isothermal sound speed extracted from the differentiation of Eq. (3).

Holmes expt.		Sesame		
P (GPa)	c_s km/s	V cm^3/mol	T (K)	c_T km/s
11.3	8.5	8.41	2418	6.8
19.7	8.6	7.34	4143	8.3
22.2	9.0	7.12	4619	8.7
27.3	8.9	6.72	5724	9.4

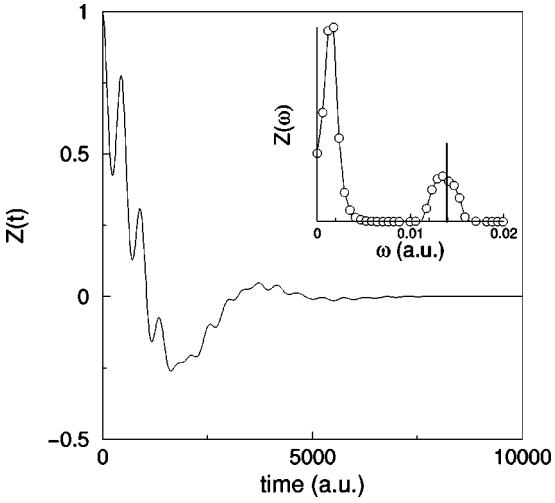

FIG. 3. Velocity autocorrelation function $Z(t)$ versus time and its spectrum $\tilde{Z}(\omega)$ versus frequency at $r_s=2$ and $T=1330$ K. The vertical line indicates the vibrational frequency for deuterium $\omega=0.0138$ a.u.

IV. TRANSPORT PROPERTIES

A. Protons self-diffusion

A proton self-diffusion coefficient is obtained with an excellent precision by integration of the velocity autocorrelation function $Z(t)$:

$$D=\int_0^\infty Z(t)dt \tag{5}$$

regardless of the nature of the molecular or dissociated state. All diffusion constants, given in Table III, have been translated into hydrogen units for the sake of comparison with other calculations, by multiplying D_D computed for deuterium by $\sqrt{A_D}$, where A_D is the deuterium molar mass, and are plotted on Figs. 4 and 5. The agreement with previous GGA simulations [35] is excellent. At high temperature ($T>10\,000$ K) where almost all molecules are broken, the system can be seen as a kind of strongly screened plasma. Thus, the OCP prediction

$$D^*=c\Gamma^{-\alpha} \tag{6}$$

with $c=2.95$, $\alpha=1.35$, and $\Gamma=e^2/ak_BT$ [8] strongly underestimates the diffusion constant. Recently, Murillo [22] proposed a simple way to connect dynamical properties of screened Coulomb systems to those of the OCP. Using an argument based on an equivalent hard-spheres system, Murillo suggested to inject into OCP's formulas a renormalized coupling parameter

$$\Gamma_{OCP}=A(\kappa)+B(\kappa)\Gamma+C(\kappa)\Gamma^2 \tag{7}$$

with κ being the inverse screening length in a units and

TABLE III. Thermodynamic properties and transport coefficients for three densities corresponding to $r_s=2$ ($\rho=0.665$ g/cc), $r_s=1.75$ ($\rho=1$ g/cc), and $r_s=1.5$ ($\rho=1.5$ g/cc). Diffusion and viscosity are computed in hydrogen units. The last column indicates the number of 0.2 fs time steps after thermalization.

r_s	Temperature (K)	Pressure (GPa)	Diffusion (10^4 cm^2/s)	Viscosity (10^4 Pa s)	Steps
2	792	16.7	2.2	2.	1800
	1350	19.0	3.7	3.5	1500
	3560	26.5	23	1.7	1700
	4780	25.1	38	1.6	2900
	5878	27.1	56	1.5	1600
	11 020	40.9	177	1.1	2000
	19 800	68.6	394	8.4	2000
	30 250	112.5	651	10.6	2000
	50 100	197.1	1100	9.4	2500
1.75	896	46.0	0.5	4.3	1500
	2019	53.9	3.4	5.0	1500
	3091	55.9	13	3.1	1200
	5700	61.7	60	1.4	1700
	7760	71.6	94	2.6	1500
	11 300	90.1	156	4.6	2000
	19 800	138.6	268	10.0	2000
	29 677	193.9	436	8.7	3500
	49 700	319.3	694	11.0	2000
1.5	5970	156.5	44.0		500
	7700	198.2	61.0	2.5	1250
	11 800	203.3	103.0	4.5	1500
	19 900	271.9	195.0	8.5	4000
	29 422	350.6	268.0	9.4	3000
	49 700	535.0	462.0	17.7	2000

$$A(\kappa)=\frac{0.46\kappa^4}{1+0.44\kappa^4},$$

$$B(\kappa)=1.01e^{-0.92\kappa},$$

$$C(\kappa)=-3.7\times10^{-5}+9.0\times10^{-4}\kappa-2.9\times10^{-4}\kappa^2.$$

A natural screening length in this regime is the Thomas-Fermi screening length, which in *a* units reads

$$\lambda_{TF}=\left(\frac{\pi}{12Z}\right)^{1/3}\frac{1}{\sqrt{r_s}}.$$

As shown in a previous paper [10], this length overestimates the screening and thus the diffusion coefficient. We have found that $\lambda=1/\kappa=2\lambda_{TF}$ gives diffusion coefficients in excellent agreement with simulation when used in Eqs. (7) and (6) as shown in Figs. 4 and 5.

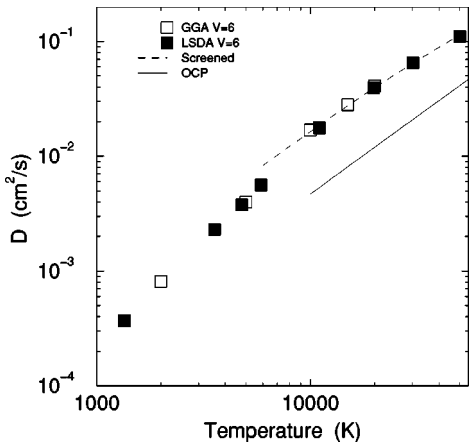

FIG. 4. LSDA proton self-diffusion constant versus temperature at $V=6$ cm^3/mole ($r_s=2$) (filled squares), compared with the GGA result (open squares [35]), the OCP formula Eq. (6) (full line), and the screened OCP formula Eq. (6) used with a coupling parameter given by Eq. (7) (dashed line).

B. Shear viscosity

The viscosity has been computed by integrating the stress-stress autocorrelation function

$$\tilde{\eta}=\frac{V}{k_BT}\int_0^{+\infty}\eta(\tau)d\tau \tag{8}$$

$$=\frac{V}{k_BT}\int_0^{+\infty}\langle\sigma^{\alpha\beta}(\tau)\sigma^{\alpha\beta}(0)\rangle d\tau, \tag{9}$$

where $\sigma^{\alpha\beta}$ are the five independent components of the traceless stress tensor: σ^{xy}, σ^{yz}, σ^{zx}, $\frac{1}{2}[\sigma^{xx}-\sigma^{yy}]$, and $\frac{1}{2}[\sigma^{yy}-\sigma^{zz}]$ with

$$\sigma^{\alpha\beta}=\sum_i m_i v_i^\alpha v_i^\beta+\sum_i\sum_{j\neq j} r_{ij}^\alpha F_{ij}^\beta, \tag{10}$$

where m_i and v_i^α are the masses and the $\alpha=x$, y, or z component of the velocity of the ith particle and r_{ij}^α, F_{ij}^β the α

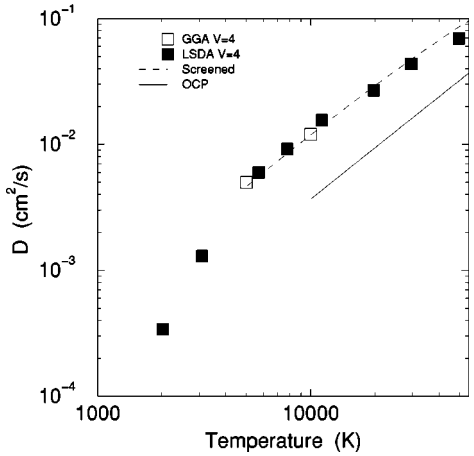

FIG. 5. Same as Fig. 4 for $V=4$ cm^3/mole ($r_s=1.75$).

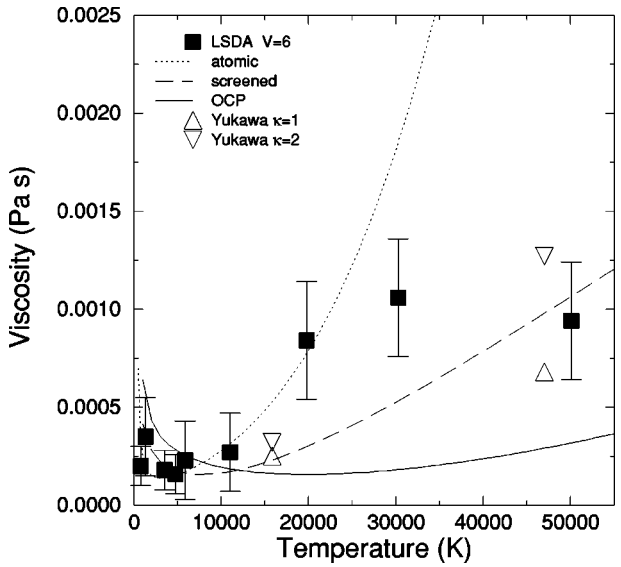

FIG. 6. LSDA shear viscosity in Pa s versus temperature at $V=6$ cm^3/mole ($r_s=2$) (filled squares), compared with the OCP formula Eq. (6) (full line) and the screened OCP formula Eq. (6) used with a coupling parameter given by Eq. (7) (dashed line). The dotted line is the fit obtained from the classical model given by Eq. (1).

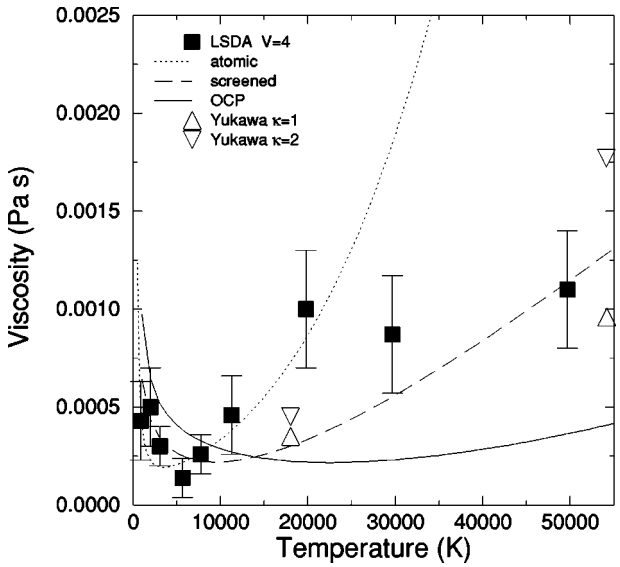

FIG. 7. Same as Fig. 6 for $V=4$ cm^3/mole ($r_s=1.75$).

and β component of the distance and of the force between i and j. Shear viscosity is a difficult quantity to extract from *ab initio* simulations because it requires very long simulations to get rid of statistical noise. Nevertheless, estimations of the viscosity of liquid aluminum and iron-sulfur alloy have been obtained by this technique by Alfe and Gillan [36] after very long simulations of more than 2×10^4 time steps for 64 particles. In our case, we are aware that our simulations are very short compared to the previous one (see Table III) and thus stress-stress autocorrelations functions are much more noisy as shown in Fig. 6. At low temperature ($T<5000$ K) a strong coupling between shear modes and vibrational modes is revealed by the frequency analysis of the stress-stress autocorrelation [Fig. 6(a)], leading to a unexpectedly low value of the viscosity just before the freezing of the system ($T=792$ K at $r_s=2$ or $T=896$ K at $r_s=1.75$). A simple atomic system would have seen a strong increase of the viscosity under the same conditions.

C. Estimation of errors bars

From the inspection of Fig. 6 it appears that after a first well-defined decay, a level of statistical noise remains that has no physical meaning. To get rid of this noise we have killed the signal after some cutoff time by multiplying it by a Gaussian function (dashed line in Fig. 6). Clearly, this procedure tends to underestimate the viscosity. Oppositely, we have also replaced the the original signal by an algebraic tail after some cutoff time, which overestimates the viscosity. Errors bars were estimated in the following way. We integrate Eq. (8) by trapezoidal rule:

$$\tilde{\eta}=\frac{1}{2}\eta(0)+\Delta t\sum_{n=1}^{nmax}\eta(n\cdot\Delta t), \tag{11}$$

which splits the viscosity into two contributions: a initial shear modulus $\eta(0)$ and a tail contribution. Hence the relative error can be written

$$\frac{\Delta\tilde{\eta}}{\tilde{\eta}}=\frac{1}{2}\frac{\Delta\eta(0)}{\eta(0)}+\frac{\Delta\eta_{\text{tail}}}{\eta_{\text{tail}}}. \tag{12}$$

The first term is the error on $\eta(0)$ which can be evaluated from the standard deviation of block averages computed over 400 time steps. The error on the tail contribution can be estimated by the comparison between the two treatments of noise at long time as described before. By adding those two kind of errors we get relative errors in the range 20%$-$ $-$30%, which, taking into account our small number of integration steps (2000–4000 time steps), can be considered as acceptable and can still indicate physical trends.

D. Comparisons with theoretical models

For each molar volume, we have plotted the value of the viscosity predicted by the classical atomic model Eq. (1) and by the OCP model as given by the Wallenborn-Baus formula [9]:

$$\eta^*=\lambda I_1+\frac{(1+\lambda I_2)^2}{\lambda I_3}, \tag{13}$$

where

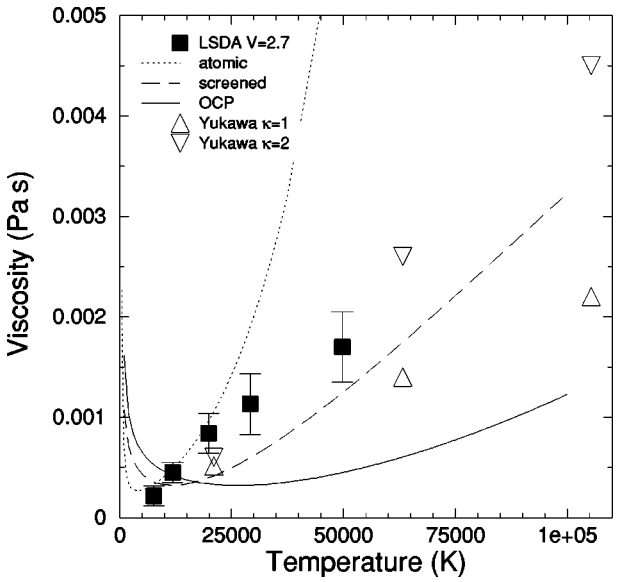

FIG. 8. Same as Fig. 6 for $V=2.7$ cm^3/mole ($r_s=1.5$). Note the extended scale to show Yukawa simulations at $\Gamma=2$ ($T=105\,300$ K).

$$\lambda=\frac{4\pi}{3}(3\Gamma)^{3/2},$$

$$I_1=(180\Gamma\pi^{3/2})^{-1};$$

$$I_2=\frac{0.49-2.23\Gamma^{-1/3}}{60\pi^2},$$

$$I_3=0.241\frac{\Gamma^{1/9}}{\pi^{3/2}}, \tag{14}$$

and where η^* is the dimensionless viscosity. The transformation into SI units is given by the same kind of relation than for diffusion after multiplying by the mass density (see Ref. [8]). Following the same idea as for diffusion, we have also plotted the screened viscosity (13) with a renormalized coupling parameter given by the Murillo's rule Eq. (7) and with the same screening length $\lambda=2\lambda_{TF}$ (quoted as screened model). New molecular-dynamics results on Yukawa potentials by Salin and Caillol [21] have also been computed with two screening wave numbers: $\kappa=1$ (up triangles) and $\kappa=2$ (down triangles), κ being in a unit. For the two densities we have plotted in Figs. 7 and 8 the viscosity in hydrogen units versus temperature. The transformation from deuterium simulations to hydrogen units is now $\eta_H=\eta_D/\sqrt{A_D}$.

E. Discussion

Inspection of Figs. 7 and 8 reveals that after following at first the ''atomic'' prediction given by Eq. (1) up to 20 000 K, the values of the viscosity saturate and become in better agreement with the screened plasma model with the same screening length as previously ($\lambda=1/\kappa=2\lambda_{TF}$). This transition seems to occur sooner for the highest density. Although this saturation could be attributed to the small number of

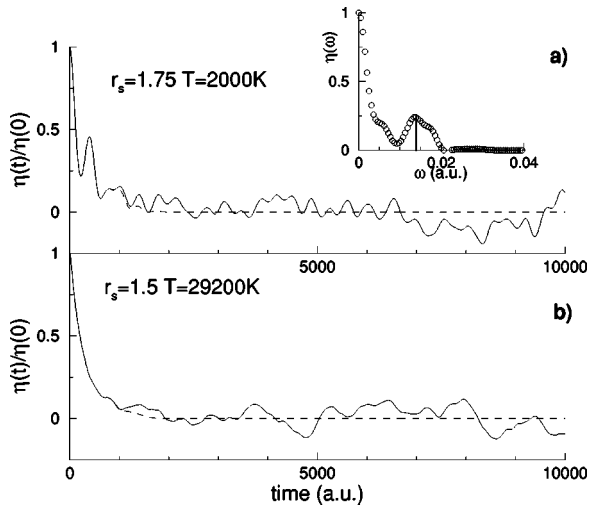

FIG. 9. Normalized autocorrelation function of the stress tensor versus time in atomic units for (a) $r_s=1.75$ and $T=2000$ K in the molecular region and (b) $r_s=1.5$ and $T=29\,000$ K in the fully dissociated regime. The inset is the frequency analysis in atomic units of the molecular stress autocorrelation function and the vertical bar indicates the vibrational frequency for deuterium.

TABLE IV. The first part of the table gives dimensionless viscosities η^* versus coupling parameter Γ for different screening parameters κ computed by Salin and Caillol [21]. The second part gives the viscosities and coupling parameters translated, respectively, in Pa s$\times10^{-4}$ and in Kelvin versus ρ for three densities corresponding to Figs. 7, 8, and 9. For each density, we give the OCP result ($\kappa=0$) given by the Wallenborn and Baus formula [9], the results of Salin and Caillol for two screening parameters ($\kappa=1$ and $\kappa=2$) , and the Murillo's formula [22] for $\kappa=1$. The value for $\Gamma=3.3$ has been interpolated.

$\kappa\downarrow$ $\Gamma\rightarrow$	10	3.3	2
0	0.073	0.131	0.291
1	0.1122	0.304	0.496
2	0.1451	0.568	0.991
3	0.1982	0.393	1.282

r_s	ρ	T(K)$\rightarrow$	$\kappa\downarrow$	15 800	47 000	79 000
		WB	0	1.63	2.9	6.5
2	0.337	Salin	1	2.5	6.8	11.
		Salin	2	3.2	13	22
		Murillo	1	2.1	8.8	17
		T(K)$\rightarrow$	$\kappa\downarrow$	18 000	54 100	90 300
1.75	0.5	WB	0	2.3	4.1	9.1
		Salin	1	3.5	9.5	16
		Salin	2	4.5	18	31
		Murillo	1	2.9	13	24
		T(K)$\rightarrow$	$\kappa\downarrow$	21 063	63 180	105 300
1.5	0.8	WB	0	3.3	6.0	13.3
		Salin	1	5.1	14	22
		Salin	2	6.7	26	45
		Murillo	1	4.3	18	36

simulated particles, as pointed out by Sanbonmatsu and Murillo [37], we would rather think that this effect is the indication of a crossover between an atomic behavior and a screened plasma behavior.

In order to test this ''atomic'' hypothesis we have performed extra simulations at $r_s=1.5$, $V=2.7$ cm^3/mole corresponding to $\rho=1.5$ g/cm^3 for deuterium. Results are shown on Fig. 9. It appears clearly that the atomic solution is no longer a reasonable prediction even at 20 000 K. On the contrary, the screened model is more coherent with the viscosity data, which confirms the hypothesis of a direct transition from the molecular regime to the screened plasma regime. Moreover, our results at high temperature ($T \geqslant 30\,000$ K) are bracketed by Salin's Yukawa simulations for screening parameter κ equal to 1 and 2, which corresponds to screening lengths between $2\lambda_{TF}$ and λ_{TF} (see Table IV, where dimensionless units have been translated into SI units).

We believe that at ''low'' density ($\rho=0.1$ g/cm^3) we would observe the opposite effect due to the existence of a well-defined atomic phase. But simulations for such a system are prohibitively expensive. One could ask why such a crossover between atomic and plasma behavior does not appear on the diffusion constant? Our explanation is that diffusion is a rather simple quantity with a monotonic behavior in contrast with the viscosity that is a nonmonotonic quantity.

V. CONCLUSION

In this paper we have presented new results on sound speed and transport coefficients of deuterium computed with *ab initio* simulations in the local spin-density approximation. From the computed equation of state in the molecular phase we have derived sound speed values in excellent agreement with recent experimental results [32]. In the dissociated phase, the diffusion constant has been interpreted in the light of a screened plasma model [22] with a very good agreement. In the same regime, the behavior of the viscosity versus temperature reveals a crossover from an atomic regime to the screened plasma model, which was not observed with the diffusion constant. The agreement between our simulations data with Murillo's and with recent Yukawa simulations of Salin and Caillol [21] indicates that the dimensionless inverse screening length κ lies between 1 and 2, which confirms the value given by diffusion coefficients. If the Thomas-Fermi screening length is multiplied by a factor of 2, we get a screening parameter κ (in units a) equal to 1.105 at $r_s=2$ and 0.9572 at $r_s=1.5$. The use of the finite temperature Thomas-Fermi screening length slightly increases the interactions (increases the screening length) but cannot reproduce our renormalization factor of 2, which confirms that screening is strongly nonlinear in the case of hydrogen due to the lack of core electrons. Higher-temperature simulations ($T>50\,000$ K) would be highly desirable to go further in the dissociated regime and to validate Murillo's screening approach, but we consider that 50 000 K is a practical limit due to the large number of excited states to be considered. At higher temperatures, for a fully dissociated system, simpler models such as (Thomas-Fermi molecular dynamics) should be able to take over to predict transport properties as shown for the pressure [38]. Finally, simulations at lower density ($V=7$ and $V=8$ cm^3/mole) are needed to compare with gas gun experiments and also to validate the existence of a broader atomic regime leading to much higher values of the viscosity.

ACKNOWLEDGMENTS

We thank Dr. N. Holmes for kindly sending sound velocities data in deuterium and also G. Salin and J. M. Caillol for giving us molecular-dynamics data on Yukawa systems. We wish also to acknowledge P. Loubeyre, G. Chabrier, G. Zérah, J. B. Maillet, and S. Bernard for fruitful discussions.

[1] S. Bagnier, P. Blottiau, and J. Clérouin, Phys. Rev. E **63**, 015301(R) (2001).
[2] T.J. Lenosky, S.R. Bickham, J.D. Kress, and L.A. Collins, Phys. Rev. B **61**, 1 (2000).
[3] G. Galli, R.Q. Hood, A.U. Hazi, and F. Gygi, Phys. Rev. B **61**, 909 (2000).
[4] B. Militzer and E.L. Pollock, Phys. Rev. E **61**, 3470 (2000); B. Militzer and D.M. Ceperley, Phys. Rev. Lett. **85**, 1890 (2000).
[5] L.B. DaSilva, P. Celliers, G.W. Collins, K.S. Budil, N.C. Holmes, T.W. Barbee, Jr., B.A. Hammel, J.D. Kilkenny, R.J. Wallace, M. Ross, R. Cauble, A. Ng, and G. Chiu, Phys. Rev. Lett. **78**, 483 (1997).
[6] G.W. Collins, L.B. DaSilva, P. Celliers, D.M. Gold, M.E. Foord, R.J. Wallace, A. Ng, S.V. Weber, K.S. Budil, and R. Cauble, Science **281**, 1178 (1998).
[7] P.M. Celliers, G.W. Collins, L.B. DaSilva, D.M. Gold, R. Cauble, R.J. Wallace, M.E. Foord, and B.A. Hammel, Phys. Rev. Lett. **84**, 5564 (2000).
[8] J.P. Hansen, I.R. McDonald, and E.L. Pollock, Phys. Rev. A **11**, 1025 (1975). The diffusion constant is given in plasma units $a^2\omega_p$. The transformation into cm^2/s is given by $D_{\mathrm{cm}^2/\mathrm{s}} = 0.04684 r_s^{1/2} D^*$ for fully ionized hydrogen plasma.
[9] J. Wallenborn and M. Baus, Phys. Rev. A **18**, 1737 (1978).
[10] G. Zérah, J. Clérouin, and E.L. Pollock, Phys. Rev. Lett. **69**, 446 (1992).
[11] J.G. Clérouin and S. Bernard, Phys. Rev. E **56**, 3534 (1997).
[12] J. Kohanoff and J.P. Hansen, Phys. Rev. E **54**, 768 (1996).
[13] I. Kwon, J.D. Kress, and L.A. Collins, Phys. Rev. B **50**, 9118 (1994); L.A. Collins, I. Kwon, and J.D. Kress, N. Trouiller, and D. Lynch, Phys. Rev. E **52**, 6202 (1995).
[14] A. Alavi, M. Parrinello, and D. Frenkel, Science **269**, 1252 (1994).
[15] M.O. Robbins, K. Kremer, and G.S. Grest, J. Chem. Phys. **88**, 3286 (1988).
[16] R.T. Farouki and S. Hamaguchi, J. Chem. Phys. **101**, 9885 (1994); S. Hamaguchi and R.T. Farouki, *ibid.* **101**, 9876 (1994); S. Hamaguchi, R.T. Farouki, and D.H. Dubin, *ibid.* **105**, 7641 (1996).

[17] J.M. Caillol and D. Gilles, J. Stat. Phys. **100**, 905 (2000).
[18] Y. Rosenfeld, Mol. Phys. **88**, 1357 (1996).
[19] G. Salin and J.M. Caillol, J. Chem. Phys. **113**, 10 459 (2000).
[20] H. Ohta and S. Hamaguchi, Phys. Plasmas **7**, 4506 (2000).
[21] G. Salin and J. M. Caillol (unpublished).
[22] M.S. Murillo, Phys. Rev. E **62**, 4115 (2000).
[23] A. Nagy, Phys. Rep. **298** (1998).
[24] G. Kresse and J. Hafner, Phys. Rev. B **47**, R558 (1993); G. Kresse and J. Furthmüller, Comput. Mater. Sci. **6**, 15 (1996); Phys. Rev. B **54**, 11 169 (1996).
[25] D. Vanderbilt, Phys. Rev. B **41**, 7892 (1990).
[26] J.P. Perdew, in *Electronic Structure of Solids*, edited by F. Ziesche and H. Eschrig (Akademie Verlag, Berlin, 1991).
[27] J.F. Dufrêche and J. Clérouin, J. Phys. IV **10**, Pr5-303 (2000).
[28] M. Ross, Phys. Rev. B **58**, 669 (1998).
[29] M. Ross, F. Ree, and D. Young, J. Chem. Phys. **79**, 1487 (1983).
[30] F. Ree, in *Shock Waves in Condensed Matter*, edited by S.C. Schmidt and N.C. Holmes (Elsevier, New York, 1987), p. 125.
[31] P. Loubeyre, R. LeToullec, D. Hausermann, M. Hanfland, R.J. Hemley, H.K. Mao, and L.W. Finger, Nature (London) **383**, 702 (1996).
[32] N. Holmes (unpublished).
[33] G.I. Kerley, in *Molecular Base Study of Fluids*, edited by J.M. Haile and G.A. Mansoori (American Chemical Society, Washington, D.C., 1983), pp. 107–138.
[34] G. Pratesi, L. Ulivi, F. Barocchi, P. Loubeyre, and R. Le Toullec, J. Phys.: Condens. Matter **9**, 10 059 (1997).
[35] L.A. Collins, S.R. Bickham, J.D. Kress, and S. Mazevet, T.J. Lenosky, N.J. Troullier, and W. Windl, Phys. Rev. B **63**, 184110 (2001).
[36] D. Alfe and M.J. Gillan, Phys. Rev. Lett. **81**, 5161 (1998).
[37] K.Y. Sanbonmatsu and M.S. Murillo, Phys. Rev. Lett. **86**, 1215 (2001).
[38] J.I. Penman, J.G. Clérouin, and P.G. Zérah, Phys. Rev. E **51**, R5224 (1995).